



## Cooling High Power Microchip Using Metallic Porous Heat Sink

Sabah F. H. Alhamdi<sup>1\*</sup>, Mohammad M. S. Al Azawii<sup>2</sup> and Ahmed K. Alshara<sup>3\*</sup>

Department of Mechanical Engineering, University of Misan, Amarah, Misan 62001, Iraq

### ARTICLE INFO

#### Article history:

Received August 28, 2024

Revised January 5, 2025

Accepted January 10, 2025

Available online March 1, 2025

#### Keywords:

High-power microchip

Porous metallic media

Heat sink

Numerical analysis

### ABSTRACT

Modern living and technological advancements demand high-power microchips, leading to an increase in chip surface temperatures. To mitigate this heat, porous metallic heat sinks are employed. This study presents a simulation of a high-power microprocessor ( $>10^4$  W/m<sup>2</sup>) encased in a porous metallic heat sink. The microchip measures 4 cm in diameter with a thickness of 5 mm. The governing equations are solved numerically using the finite element method, implemented in COMSOL Multiphysics software. This paper investigates the cooling performance of a microchip through natural convection, focusing on three key parameters: aspect ratio, porosity, and heat sink material. The study considers heat sink porosities of 0.2, 0.4, and 0.8; aspect ratios of 0.2, 0.5, 1, and 2; and heat sink materials including copper, aluminium, and steel. Results are presented as temperature and Nusselt number contours on the microchip's surface. The findings indicate that copper achieves the lowest surface temperature (41.58°C) and the highest Nusselt number (243.81) at an aspect ratio of 2. Increasing the aspect ratio enhances the heat transfer rate and, consequently, the Nusselt number. Conversely, steel exhibits the highest surface temperature (89.35°C), the lowest heat transfer coefficient (164.89 W/m<sup>2</sup>·K), and the lowest Nusselt number (62.84).

## 1. Introduction

Electronic devices have become the driving force of modern living, in which the use of small-sized, faster and more powerful equipment have increased in the global marketplace. Therefore, a high level of performance in electronic devices is a prioritized feature that the electronic industry needs to develop [1]. The heat generated in the microchip affects the efficiency of the electronic device, and thus decreased their operational life span [2]. To reduce the temperature in the electronic device components, the generated heat should be dissipated to the ambient [2, 3] in order to maintain the operating temperature of microchip at less than 85°C to thus ensure high performance [4]. Due to the small size, compact design and fast processing of recent electronics such as micro-processor, the generated heat flux

has increased [1], with heat flux exceeding 1000 W/cm<sup>2</sup> in some spots [4], leading to high temperature which should be removed or cooled down. Conventional methods used to cool electronic devices include forced air cooling [5], various alternative methods like heat pipe [6], phase change materials (PCM) [7] thermoelectric cooling [8], and microchannels. However, these typical cooling methods are often not effective [9]. Heat sinks could be utilized to dissipate the generated heat to the ambient and enhance heat transfer area, which works as heat exchanger [10-12]. Porous media heat sinks will help increase the overall surface area of the microchip and thus improve the heat transfer and remove the generated heat [13]. It was found that using porous media heat sinks to dissipate the generated heat is an effective method [1, 13]. A porous medium is a material

\* Corresponding authors.

E-mail address: [sabahalhamdi@uomisan.edu.iq](mailto:sabahalhamdi@uomisan.edu.iq)

DOI: [10.24237/djes.2025.18106](https://doi.org/10.24237/djes.2025.18106)

This work is licensed under a [Creative Commons Attribution 4.0 International License](https://creativecommons.org/licenses/by/4.0/).



containing pores (voids), in which two phases exist. The solid part of the porous material (matrix) is known as the solid phase. The voids are usually filled with fluid (liquid or gas such as water and air), allowing the flow of fluid through the material which is known as single-phase flow. A porous medium is most often characterized by its porosity which varies between 0 – 1 and permeability which is another important property of porous medium [14]. Convection heat transfer is the mode of heat transfer that has been used to cool electronics devices using heat sinks. Natural and forced-convection air cooling are the traditional modes of convective heat transfer [14-16]. Zaretabar, Asadian, and Ganji [17] analyzed heat transfer in aluminum and copper heat sinks installed on a chip of a computer using forced-convection, in which Nusselt number and heat transfer coefficient were determined and discussed. The results showed that Nusselt number increases with the rise in flow velocity and thus enhances thermal performance. PV, Giran, and Pradeep [13] studied numerically heat transfer enhancement of electronic chips using forced convection. In this study, three different cases are reported and compared to each other: the Bi-disperse porous medium heat sink, its conventional model, and forced convection without heat sink. It was found that the Bi-disperse porous medium heat sink is highly effective compared to the other two cases. Lee and Kim [18] used natural convection to enhance the heat transfer in pin-fin heat sink. Pin-fin and microchannel heat sinks are an important arrangement that could improve the thermal performance and reduce the high temperature in electronic devices [19, 20]. Zhao et al. [21] proposed an optimized geometry of micro square pin-fin heat sink to improve the performance of electronic devices. The numerical results showed that the cooling performance of micro heat sinks with the optimized square pin-fin is more effective than the cooling performance of micro column pin-fin heat sinks. Smakulski and Pietrowicz [22] reviewed the removal of high heat flux using three techniques, porous materials, microchannels and spray cooling. Gong, Zhao and Huang [23] studied the structure of the

micro-channels heat sink numerically. Traditional micro-channel (TMC, single hole jet-cooling, rectangle column fin, and double-layer micro-channel) were considered as heat sinks in their study. Results show that the structure of the microchannel heat sink is significant to the fluid flow and heat transfer, leading to improved thermal performance. Gong et al. [1] developed and analyzed numerically a micro-channel heat sink, in which a metallic porous/solid compound fins are used to dissipate chip power. The results showed that the proposed design of the heat sink enhances the cooling performance of the electronic devices efficiently. Habib and Tahir [2] proposed and analyzed a novel macro-channel ‘L-shaped’ heat sink to remove the large amount of the generated heat in the chip using free-convection heat transfer mode. The thermal performance is improved using an ‘L-shaped’ heat sink compared to the traditional porous medium heat sink design. Tu-Chieh, Hung and Yan [24, 25] developed a 3-D numerical model to analyze the impacts of six different porous configuration designs (rectangular, outlet enlargement, trapezoidal, thin rectangular, block, and sandwich distribution design) on the thermal enhancement of the porous-microchannel heat sinks. The results indicated that the sandwich and the trapezoidal designs have the best heat transfer effectiveness, cooling performance and convective performance. Tu-Chieh, Hung and Yan [26] numerically studied the performance of heat transfer of a microchannel heat sink with a sintered porous medium, with the heat transfer enhanced using a porous metallic medium. Pin-fin was used with phase change materials (PCM) to improve the cooling performance as well [27]. Phase change materials have the potential to enhance the heat transfer and control the temperature [28]. Arqam et.al [29] studied the impact of radial fin heat sink filled with PCM on the cooling performance of electronics, in which heat sink performed better based on their findings. However, the usage of PCM in thermal management is not acceptable for high heat fluxes ( $> 15$  W) [30]. Types of porous medium heat sink could influence the thermal management of the heat sink and microchip as well. Metals such as aluminum [13], copper

[1, 24, 31] and foams [21, 23] have been extensively used as heat sinks to improve the thermal performance of electronic devices. Copper has stronger properties than aluminum such as thermal conductivity, which higher than thermal conductivity of aluminum. However, copper is more expensive than aluminum [17]. Metal foam is considered a promising solution for the applications with high heat flux, in which air or water can be used as cooling fluid [1, 32-35]. Metal foam is usually fabricated from aluminum, carbon and silicon carbide [31], which provides large surface contact area and thus improves the heat transfer by convection [1]. Design pore densities and porosities of metal foam were investigated and analyzed in different studies [36-38]. Han et al. [39] has reviewed the studies on the usage of metal foam as a heat sink to remove the generated heat in the microchips. Forced [17, 40] and natural [2, 18] convections are the most common ways that have been used to cool the electronic devices using porous medium as heat sink. Free convection is a very cheap way to cool the heat sinks because no devices are needed to move the air. In the present paper, a simulation of a circular microprocessor with high power ( $<104$  W/m<sup>2</sup>) is achieved numerically to analyze the heat removal from the microchip through the use of a metallic porous media heat sink. To the best of the author's knowledge, no other cooling high power microchip systems have been considered and analyzed for different aspect ratios in the literature. Investigating the influence of aspect ratios for a range of porosities provides insights about the thermal management of microchip systems. Specific objectives are to analyze the cooling performance of a microchip by natural convection for three parameters (aspect ratio, porosity and type of heat sink) and determine the Nusselt number for all cases. These objectives are met with a computational fluid dynamics (CFD) model in COMSOL Multiphysics to simulate the thermal behavior inside the microchip and heat sink. Copper, aluminum, and steel were used as metal porous heat sink to remove the high surface temperature of the microchip. Four aspect ratios ( $H/D$  [41] =  $H/W$  = 0.2, 0.5, 1 and 2) and three porosities (0.2, 0.4

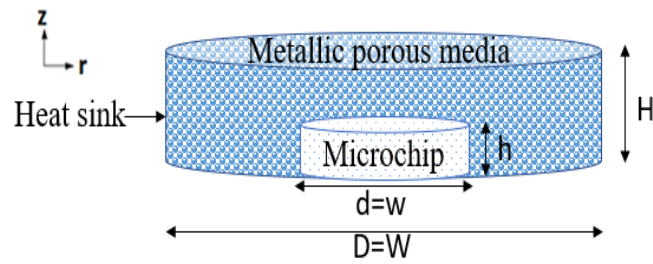
and 0.8) were used in the modeling efforts and analyzed. The electronic microchip (heat source) of 20 Watt is considered, dissipating approximately 10000 W/m<sup>2</sup> as heat flux based on the area of microchip. Contours of temperature, average surface temperature from the microchip and porous heat sink were plotted and analyzed. The Nusselt number was determined and plotted for all aspect ratios, porosities, and heat transfer coefficient.

## 2. Methodology

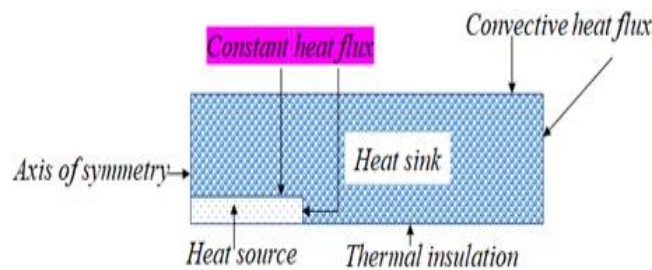
A numerical study was carried out to investigate the thermal behavior of the heat sink with three metallic porous mediums (steel, aluminum, and copper) for cooling a high-power microchip. The problem model, governing equations, corresponding boundary conditions, and numerical analysis to solve the problem are introduced.

### 2.1-Physical model of the microchip and heat sink

In this study, heat dissipation from a microchip is numerically investigated. The dimensions of the microchip are diameter  $d$  and thickness  $h$ . The microchip is surrounded with metallic porous media of porosity  $\phi$ , diameter  $D$  and thickness  $H$ . Figure (1) shows the schematic diagram of the microchip and heat sink. Three types of metal heat sink are considered in the present study: copper, aluminum and steel. The dimensions of the microchip, heat sink, and other parameters used in the study are listed in Table (1). The generated heat in the microchip is removed using metal porous medium and then dissipated by means of free convection to the surrounding. Air is used as the working fluid with Prandtl number of 0.7. The fluid flow in the porous media is considered two-dimensional, steady state, Newtonian, incompressible, and with constant thermophysical properties except the density obeys to Boussinesq approximation. The porous medium is homogenous, rigid, isotropic, and fully saturated with fluid. The local thermal equilibrium is considered between the solid and the air inside the porous media. The influence of radiation heat transfer is minimal and can be neglected based on the calculated surface temperature of the heat sinks.



(a) Dimensions of the microchip and heat sink



(b) Front view of the microchip and heat sink showing the boundary conditions

**Figure 1.** Schematic diagram of the microchip and heat sink, showing the dimensions and boundary conditions

**Table 1:** Dimensions and Parameters of the physical model used in the modeling efforts [1, 9, 31]

Sizing of Microchip and Heat sink			
Parameter	Value	Unit	
Diameter of microchip (w)	4	cm	
Height of microchip (h)	0.5	cm	
Diameter of the heat sink (W)	10	cm	
Height of heat sink (H)	2	cm	
Porosity	0.2, 0.4 and 0.8	-	
	$1.2416 \times 10^{-12}$		
Permeability	$1.7658 \times 10^{-11}$ and	$m^2$	
	$1.2714 \times 10^{-9}$		
Heat flux	$10^4$	$W/m^2$	
Aspect ratio (H/W)	0.2, 0.5, 1, and 2	-	
Thermophysical Properties of Metal Porous Mediums			
Parameter	Value	Unit	
	Steel		
Heat capacity	475	$J/(kg.K)$	
Thermal conductivity	44.5	$W/(m.K)$	
Density	7850	$kg/m^3$	
	Aluminium		
Heat capacity	900	$J/(kg.K)$	
Thermal conductivity	238	$W/(m.K)$	
Density	2700	$kg/m^3$	
	Copper		
Heat capacity	385	$J/(kg.K)$	
Thermal conductivity	400	$W/(m.K)$	
Density	8960	$kg/m^3$	

## 2.2. Governing equations and boundary conditions

Local thermal equilibrium between the solid and fluid phases inside the porous domain is assumed to analyse the heat transfer [1]. The Forchheimer-Brinkman extended Darcy model and the one-energy equation which describe the fluid flow and heat transfer in the porous region are adopted from [14]. The general governing equations are mass, momentum, and energy: Continuity equation:

$$\nabla \cdot (\phi \rho_f V) = 0, \tag{1}$$

where  $\phi$  is porosity of metallic porous media,  $\rho_f$  is density of fluid, and  $V$  is velocity vector. Momentum equation:

The characteristics of the flow and heat transfer for the air in the porous media are based on the volume-averaged technique and Brinkman–Darcy-Forchheimer model of porous media. With the above assumptions, the momentum equation of the porous media can be written as follows [14, 24]:

$$\frac{\rho_f}{\phi^2} (\nabla \cdot V) V = -\nabla P + \frac{\mu}{\phi} \nabla^2 V - \frac{\mu}{K} V - \frac{C_f \rho_f}{K^{\frac{1}{2}}} |V| V + \rho_f g \beta (T - T_\infty), \tag{2}$$

where  $P$  is pressure,  $\mu$  is viscosity of fluid,  $K$  is permeability of porous medium,  $C_f$  is Forchheimer’s constant,  $g$  is gravity, and  $\beta$  is thermal expansion coefficient of fluid.

Note that the permeability defined as Kozeny’s equation [14],

$$K = \frac{d_p^2 \phi^3}{150*(1-\phi)^2}, \tag{3}$$

where  $d_p$  is mean particle diameter.

Forchheimer’s constant is calculated from the following relation [14]:

$$C_f = 0.55 \left( 1 - 5.5 \frac{d_p}{D_e} \right), \tag{4}$$

where  $d_p$  is the mean particle diameter and  $D_e$  is the equivalent diameter of the porous media.

Energy equation:

The energy equation of fluid and porous media is [24]:

$$(\rho c)_{eff} (V \cdot \nabla T) = k_{eff} \nabla^2 T, \tag{5}$$

where  $T$  is temperature,  $k_e$  and  $(\rho c)_e$  are the effective thermal conductivity and the heat capacity of the porous media, respectively, which define as:

$$k_{eff} = \phi k_{f+} + (1 - \phi) k_s, \tag{6}$$

$$(\rho c)_{eff} = \phi (\rho c)_{f+} + (1 - \phi) (\rho c)_s. \tag{7}$$

The subscript indices  $f$  and  $s$  stand for liquid and solid, respectively.

The boundary conditions:

The corresponding boundary conditions used in the present study represent the following cases in which:

1. The bottom surfaces of the microchip and the porous media are insulated.
2. The top and side surfaces of microchip subject to constant heat flux,  $q''$ .
3. The no slip condition applies at the top and side surfaces of microchip, where  $u = v = w = 0$ .
4. Convective heat transfer with top and side surfaces of porous media with surrounding, where heat transfer coefficient is  $9.37 \text{ (W/m}^2 \cdot \text{K)}$  for still air [42].

Parameters:

Nusselt Number:

The local Nusselt number ( $Nu_n$ ) of fluid on the surfaces of microchip can be determined using the relation:

$$Nu_n = \frac{h_n L}{k}, \tag{8}$$

where  $h_n$  is the local heat transfer coefficient in the direction  $n$ , which can be estimated from the relation,

$$h_n = \frac{q''}{T_n - T_\infty}, \tag{9}$$

while the average Nusselt number ( $Nu_{avg}$ ) can be calculated from the relation:

$$Nu_{avg} = \frac{1}{L} \int_0^L Nu_n dn, \tag{10}$$

where  $L$  is the length at any direction  $n$ .

$$Nu_{avg} = \frac{\bar{h} L}{k}, \tag{11}$$

where  $L = \left(\frac{d}{4}\right)$  for the horizontal surface of the microchip and  $d$  is the diameter of the microchip [43].

$$h_n = \frac{q''}{T_n - T_\infty}, \tag{9}$$

while the average Nusselt number ( $Nu_{avg}$ ) can be calculated from the relation:

$$Nu_{avg} = \frac{1}{L} \int_0^L Nu_n dn, \tag{10}$$

where L is the length at any direction n.

$$Nu_{avg} = \frac{\bar{h}L}{k}, \tag{11}$$

where  $L = \left(\frac{d}{4}\right)$  for the horizontal surface of the microchip and  $d$  is the diameter of the microchip [43].

### 2.3 Numerical model

The numerical model was solved and analysed using COMSOL Multiphysics software. The model computes the temperature distribution in the computational domain (microchip and heat sink). Two-dimensional axisymmetric modelling was used. The Forchheimer-Brinkman extended Darcy model interface is used to calculate the fluid velocity and pressure fields in the heat sink. The generalized Navier-Stokes flow solutions are coupled to the energy equation throughout the porous region. The porous viscous

(permeability) and inertial (Forchheimer Drag coefficient) terms are included in the model. The density obeys Boussinesq approximation. The effect of gravity is included in the model to achieve natural convection heat transfer to the surrounding. The permeability and porosity are given in Error! Reference source not found.) in the previous section [1, 31].

### 2.4 Mesh validation

The mesh size used in the model was extremely fine (free Triangular). The numerical model is solved for nine different mesh types to find an accurate mesh type. **Error! Reference source not found.** a show the surface temperature of the microchip with aluminium as heat sink ( $z = 0.5$  cm and  $r = 0 - 2$  cm for the nine eight different mesh sizes at  $AR = 0.2$  and  $\phi = 0.4$ ). As can be seen the change in the surface temperature for all mesh sizes are very small. Extra and extremely fine meshes show an excellent convergence. Extremely fine mesh is selected in the present study to get accurate results, which is shown in **Error! Reference source not found. b**.

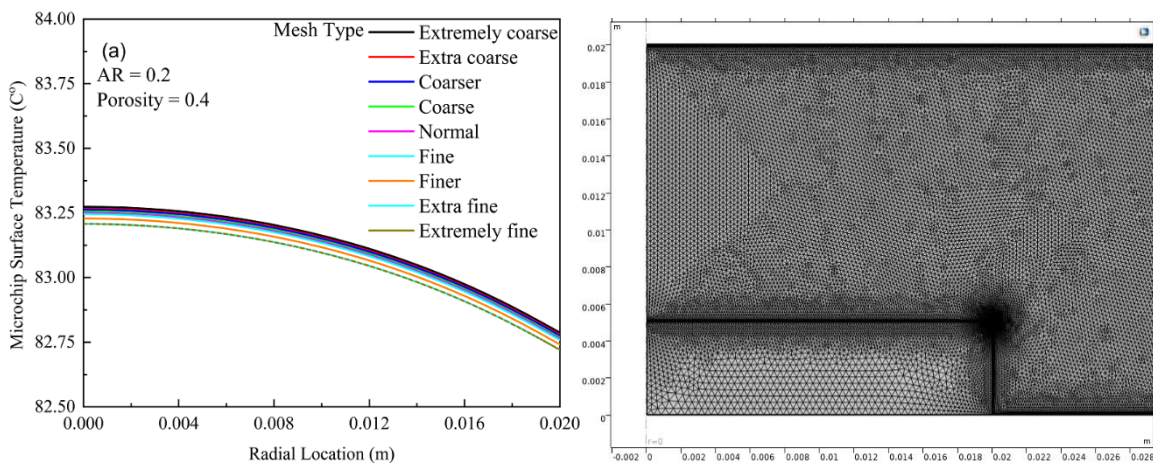


**Figure 2. (a)** The influence of mesh size on the microchip surface temperature with aluminium as heat sink.

**(b)** Zoomed-in extremely fine mesh generated by COMSOL Multiphysics model, showing the microchip and heat sink.

### 2.5 The model validation

To validate the present model, Nusselt number for a range of heat flux was compared to Nusselt number from a correlation ( $Nu = 0.54Ra^{1/4}$ ) by Pitts and Sissom [44]. The present model was run for a range of heat

fluxes (10000 to 27000  $W/m^2$ ) with very low porosity (0.99) to simulate the problem without porous media as an approximation. **Error! Reference source not found.** shows Nusselt number verse heat flux for the present study and reference [44] at aspect ratio of 0.2 for steel.

Rayleigh number (Ra) is calculated from equation (12):

$$Ra = \frac{g\beta q'' L_c^4}{k\alpha\nu} \quad (12)$$

where:  $g$  is acceleration due to gravity,  $\beta$  is the thermal expansion coefficient,  $q''$  is the uniform surface heat flux,  $L_c$  is the characteristic length,  $k$  is the thermal conductivity,  $\alpha$  is the thermal diffusivity, and  $\nu$  is the kinematic viscosity.

As can be seen in **Error! Reference source not found.**, the standard deviation between the Nusselt number from the present model and from reference [44] is in the range of (5 to 12)% which considered reasonable due to the approximation.

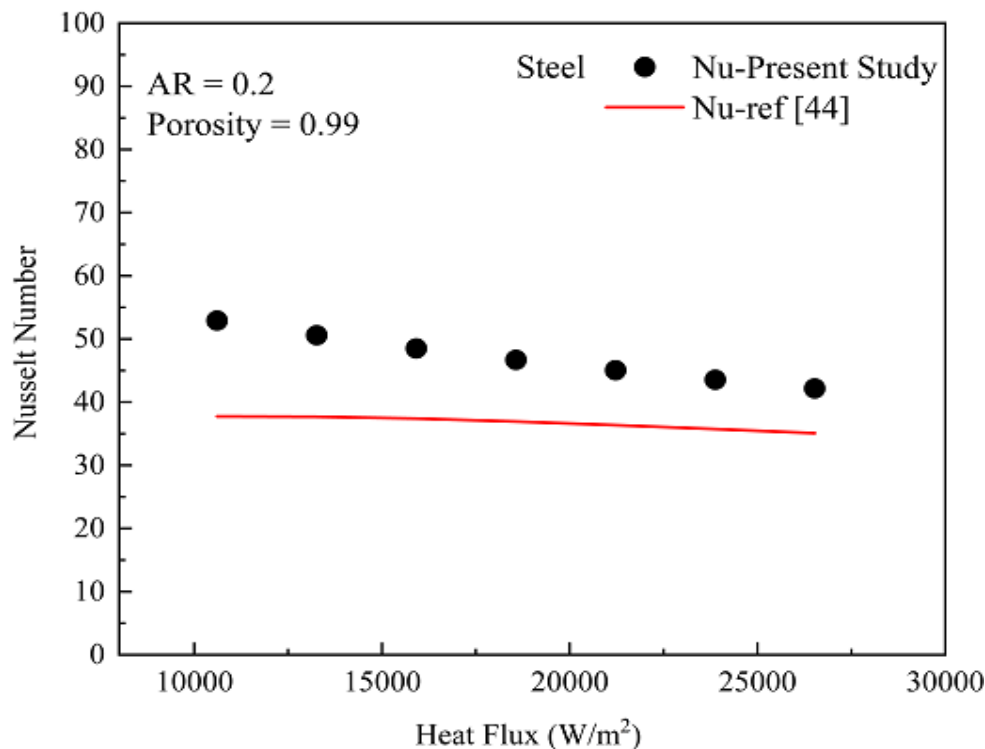


**Figure3.** Validation between the present study and reference [44] results at aspect ratio of 0.2 with steel as metallic porous domain

### 3. Results and discussion

This section focuses on the thermal behaviour of the heat sink. The impact of three types of metal heat sink is analysed. Three porosities of the porous domain are used. Furthermore, one parameter was introduced and analysed, which is the Nusselt number.

#### 3.1 Impacts of metallic porous media on the temperature distribution in the microchip and heat sink:

The problem was modelled and solved numerically. The investigation focuses on the heat transfer behaviour of the metallic porous media, in which heat transfer occurs in natural convection. The metal porous media will help to

remove the generated heat in the microchip to the ambient via convection. The surface area of the heat source (microchip) and heat sink will affect the total heat transfer by convection mode; the heat transfer will increase with the increase in surface area. Four aspect ratios, (0.2, 0.5, 1, and 2), were considered at three porosities, (0.2, 0.4 and 0.8). Figures (4) (a-f) show the temperature distribution in the microchip and the heat sink for the three metallic porous mediums, (steel, aluminium, and copper), in which aspect ratio equals 0.2 and porosity equals 0.8. Two plots are shown for each porous medium, temperature profile (contours) in Z-R sections (a, c, and e) and surface temperatures (b, d, and f). The surface temperature of the microchip and heat sink

increases with porosity due to the increase of surface area and void spaces which increase the heat transfer rate [45]. As can be seen, the copper porous medium gives the minimum temperature on the surface of the microchip ( $\sim 82.78^\circ\text{C}$ ) and heat sink ( $\sim 82.06^\circ\text{C}$ ), leading to the highest Nusselt number. This is because the copper has high thermal conductivity ( $\sim 400 \text{ W/m K}$ ) [31] compared to the other metallic heat sinks. The average surface temperature of the microchip is used to calculate the heat transfer

coefficient based on the constant heat flux and ambient temperature. Copper shows the highest heat transfer coefficient ( $183.63 \text{ W/m}^2 \text{ K}$ ) and thus the highest Nusselt number (69.98) compared to steel and aluminium. The heat transfer coefficients and Nusselt numbers are 164.89 ( $\text{W/m}^2 \text{ K}$ ) and 62.84 for steel, and 180.62 ( $\text{W/m}^2 \text{ K}$ ) and 68.83 for aluminium, respectively. Therefore, steel performs more poorly than aluminium and copper, which has the lowest thermal conductivity ( $\sim 44.5 \text{ W/m K}$

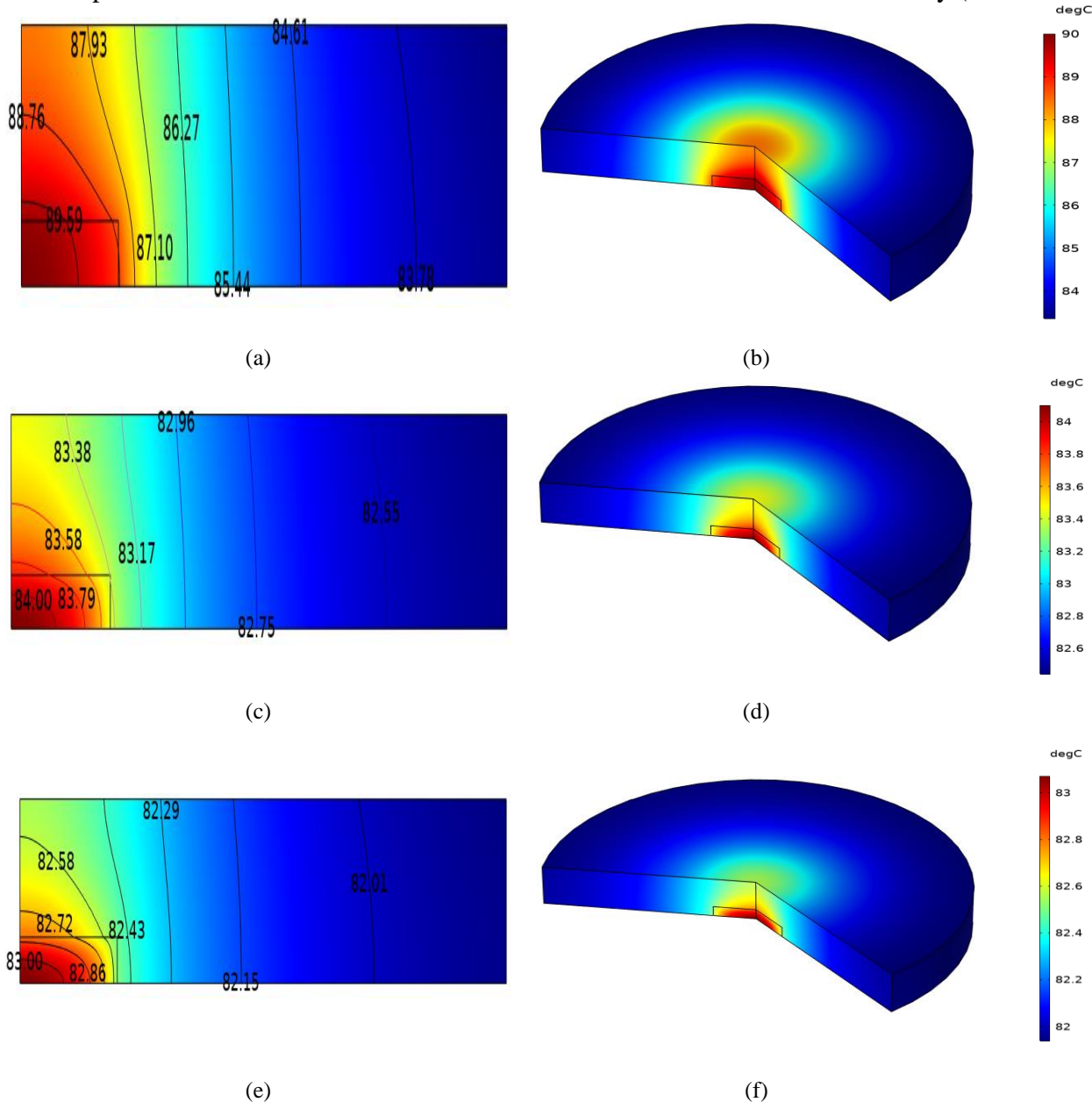


**Figure 1.** Temperature distribution in the microchip and the heat sink. a, c and e show temperature profile (contours) in Z-R section. b, d, and f show the surface temperature. a-b for steel, c-d for aluminium and e-f for copper. The aspect ratio equals 0.2

### 3.2 Effects of aspect ratio on the temperature distribution in the microchip and heat sink

Figure (5) shows the average surface temperature from the microchip and the heat sink for the three metallic porous media at four different aspect ratios and three porosities. The aspect ratio depends on the width (diameter) and height of the heat sink. Four values of aspect ratios were investigated by changing the height of the heat sink, the width of the heat sink is set to be constant. Each plot in Figure (5) shows the maximum and minimum average surface temperature in the microchip and heat sink. As can be observed in Figure (5), the maximum average surface temperature (89.35°C) is obtained from steel at porosity of 0.8 with aspect ratio of 0.2. The minimum surface temperature (41.58°C) is obtained from copper at porosity of 0.2 with aspect ratio of 2. The behaviour of the

heat sink is enhanced by increasing the aspect ratio from 0.2 to 2 due to increase the surface area to remove the heat to the ambient, the surface temperature for the microchip is minimum for all heat sinks, leading to the highest Nusselt number. At aspect ratio of 0.2 and porosity of 0.8, the Nusselt number is minimal at 62.84. While at aspect ratio of 2 and porosity of 0.2, the Nusselt number is maximal at 243.61. Table (2) shows the temperature difference between the microchip and the ambient and the temperature difference between the microchip and the heat sink. As observed in Table (2), copper records the minimal temperature difference at low porosity. The temperature difference from the microchip and the ambient was used in equation (9) to calculate the heat transfer coefficient and the Nusselt number.

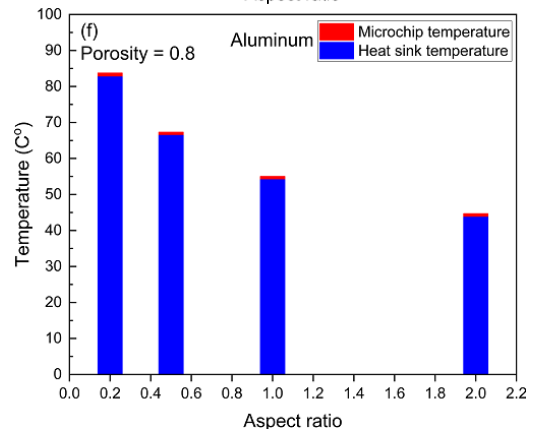
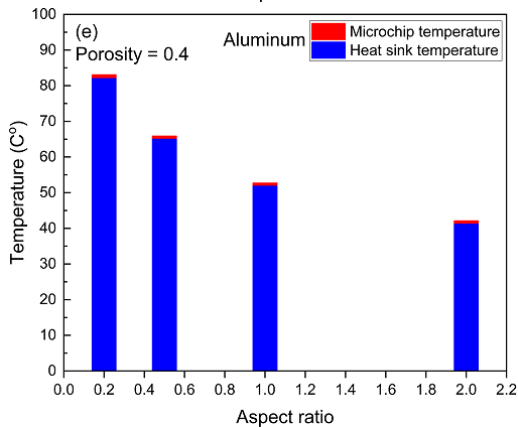
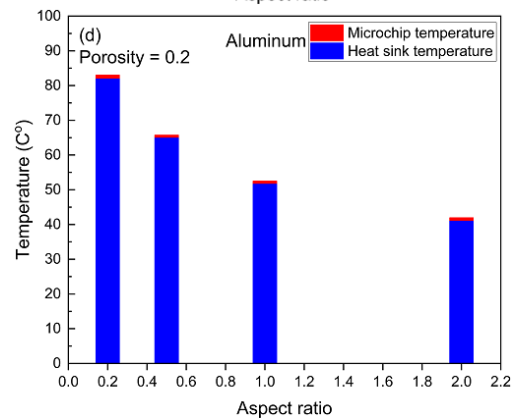
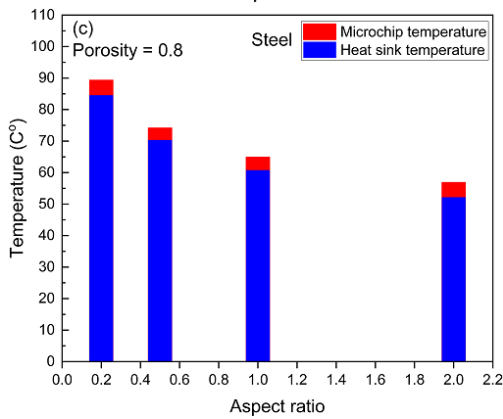
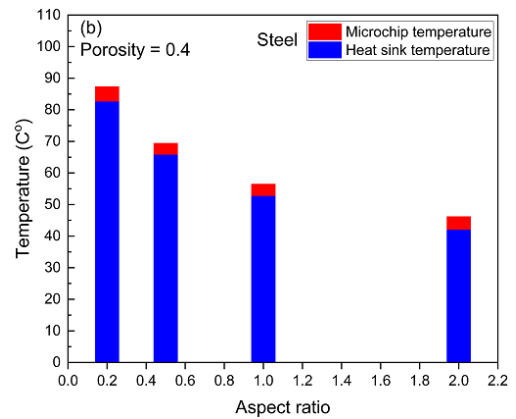
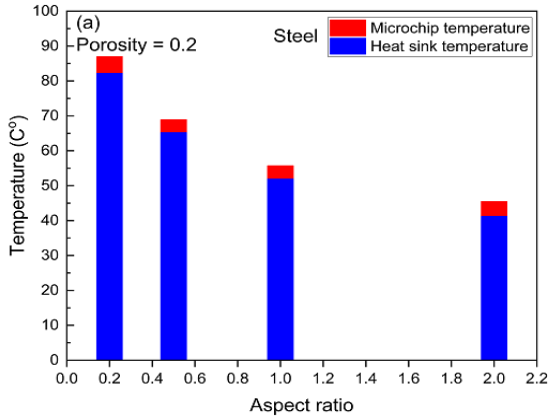
**Table 2:** Temperature difference ( $T_s - T_\infty$ ) and ( $T_s - T_b$ ) at four aspect ratios among three porosities.  $T_s$  is the average surface temperature from the microchip, and  $T_b$  is the bulk temperature or average temperature of the heat sink

Metal porous medium	Temperature difference ( $T_s - T_\infty$ ) (°C)			
	Aspect ratio ( $\phi = 0.2$ )			
	0.2	0.5	1	2
Steel	61.99	43.89	30.71	20.46
Aluminum	57.99	40.73	27.48	16.94
Copper	57.59	40.41	27.15	16.58
Metal porous medium	Temperature difference ( $T_s - T_b$ ) (°C)			
	Aspect ratio ( $\phi = 0.2$ )			
	0.2	0.5	1	2
Steel	4.78	3.71	3.82	4.25
Aluminium	1.08	0.86	0.88	0.96
Copper	0.72	0.58	0.59	0.64
Metal porous medium	Temperature difference ( $T_s - T_\infty$ ) (°C)			
	Aspect ratio ( $\phi=0.4$ )			
	0.2	0.5	1	2
Steel	62.3	44.38	31.43	21.15
Aluminum	58.09	40.88	27.71	17.15
Copper	57.62	40.45	27.21	16.64
Metal porous medium	Temperature difference ( $T_s - T_b$ ) (°C)			
	Aspect ratio ( $\phi = 0.4$ )			
	0.2	0.5	1	2
Steel	4.79	3.72	3.84	4.28
Aluminium	1.08	0.86	0.88	0.96
Copper	0.72	0.58	0.59	0.64
Metal porous medium	Temperature difference ( $T_s - T_\infty$ ) (°C)			
	Aspect ratio ( $\phi = 0.8$ )			
	0.2	0.5	1	2

	0.2	0.5	1	2
Steel	64.35	49.16	39.88	31.91
Aluminium	58.75	42.32	29.99	19.68
Copper	57.78	40.79	27.75	17.21

Temperature difference  
( $T_s - T_b$ ) (°C)  
Aspect ratio ( $\phi = 0.8$ )

	0.2	0.5	1	2
Steel	4.85	3.85	4.15	4.82
Aluminium	1.09	0.87	0.89	0.98
Copper	0.72	0.58	0.59	0.64



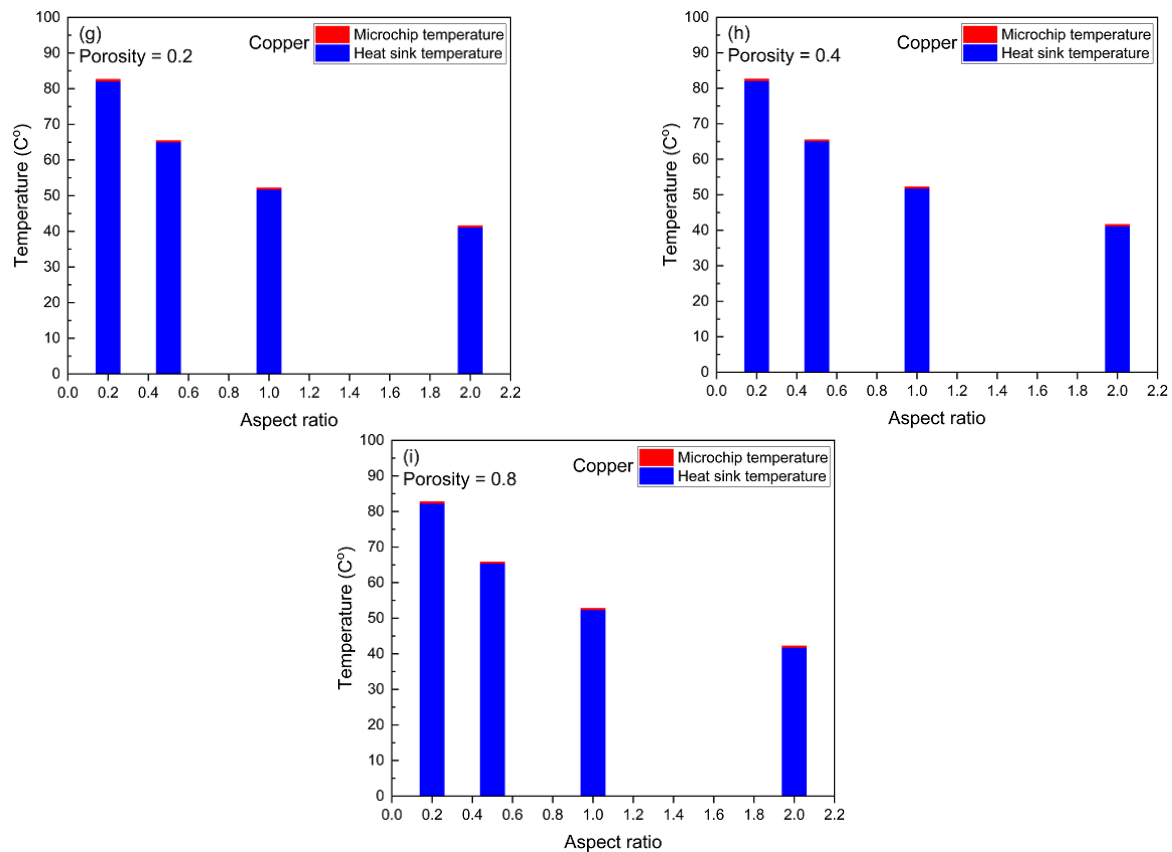


**Figure 5.** Average surface temperature from the microchip and heat sink among the three porosity values, showing the maximum and minimum temperature for aluminium, steel, and copper at four aspect ratios

### 3.3 Nusselt number formulation

The Nusselt number is a dimensionless number that represents the ratio of convective to conductive heat transfer on the surface of the microchip which is calculated using equation (11), which represent average Nusselt number [43]. In equation (11), heat transfer coefficient is calculated using equation (9) with heat flux ( $q'' = \sim 10000 \text{ W/m}^2$ ) and temperature difference from Table (2). Figure (6) shows Nusselt number vs. aspect ratio for the three metallic porous media among three porosities. Nusselt number is maximum for copper at ( $\phi = 0.2$ ) and it increases with the increase of aspect ratio as can be noticed. In addition, aluminum records better performance than steel.

Aluminum has high thermal conductivity ( $\sim 238 \text{ W/m K}$ ) [9, 31] compared to thermal conductivity of steel ( $\sim 44.5 \text{ W/m K}$ ). Therefore, large aspect ratio, low porosity and high thermophysical properties could be used to increase the heat dissipating to the ambient. Figure (7) (a-d) shows the variation of average Nusselt number with heat transfer coefficient. As can be seen, the average Nusselt number increases with the increase of heat transfer coefficient at all Aspect ratios due to the enhancement of heat transfer rate. Nusselt number for low porosity (0.2) is higher than that of high porosity (0.8) for steel, aluminum and copper.

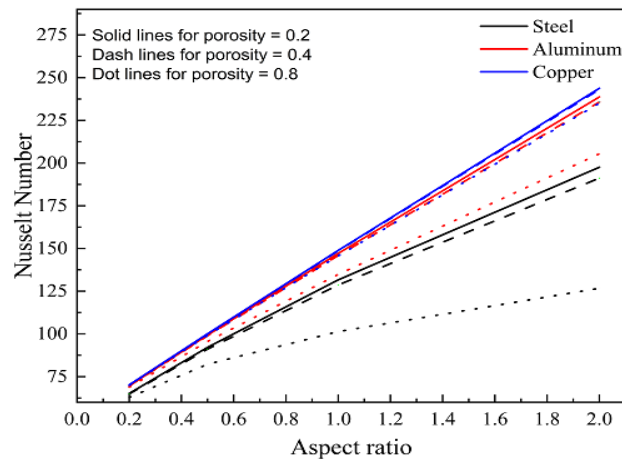


**Figure 6.** Variation of Nusselt number for the three metallic porous mediums among four different aspect ratios and three values of porosity

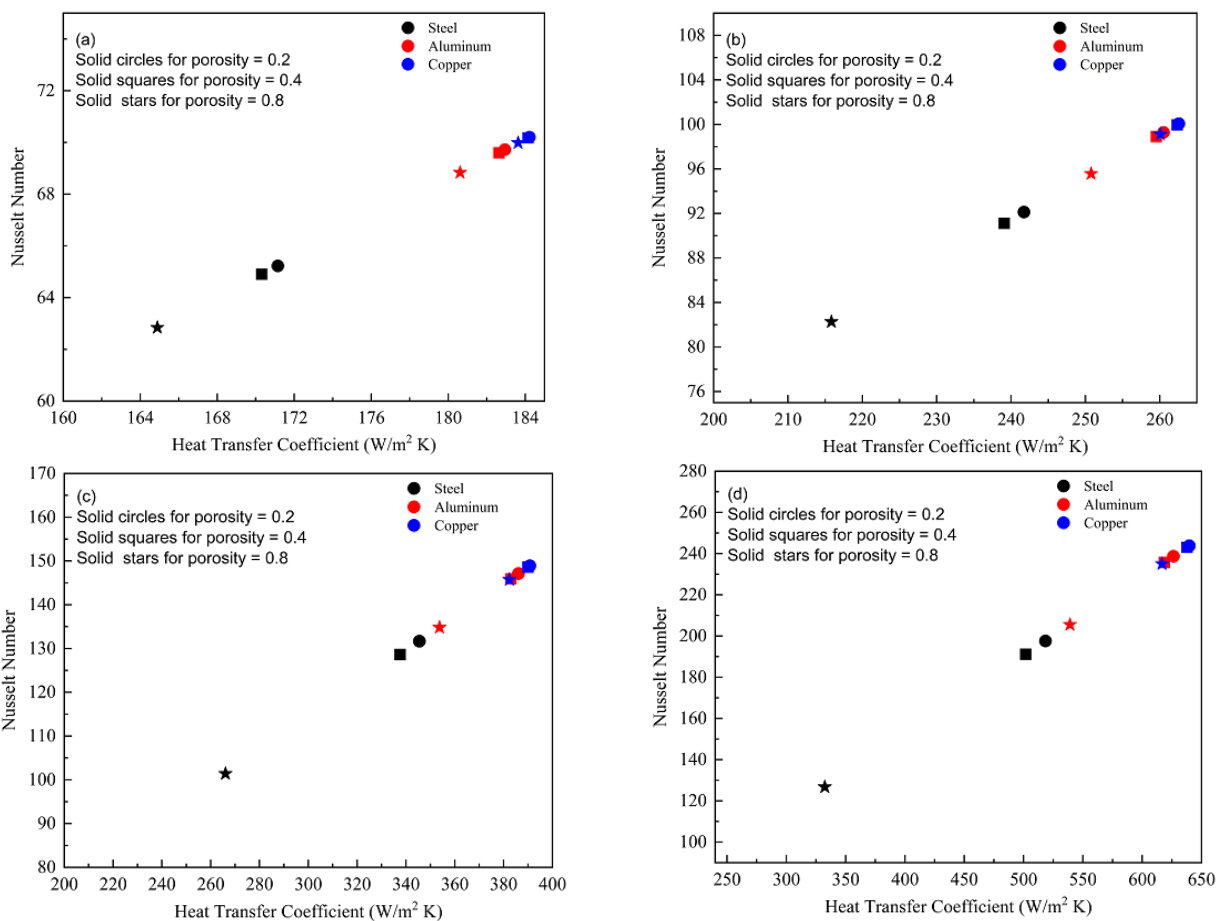


**Figure 7.** Nusselt number vs. heat transfer coefficient among three different values of porosities. (a) Aspect ratio = 0.2, (b) aspect ratio = 0.5, (c) aspect ratio = 1, and (d) aspect ratio = 2.

### 3.4 Impact of the porosity on the performance of the heat sink

In the present study, the model was run within a porosity range of 0.1 to 0.9. The impact of low porosity ~0.1-0.4 on the results is approximately the same for all heat sinks as can

be seen in Figure (8) which shows the surface temperature of the microchip along the radial direction. At high porosity 0.4-0.9, the impact of porosity on the surface temperature is very clear. Three porosities were selected (0.2, 0.4 and 0.8) in the present study in order to avoid repeating the same results. As can be observed in the

previous sections, Figures (5, 6, and 7) and Table (2), the performance of the heat sink increases with a decrease in porosity, with an enhancement of the heat transfer also. In addition, Nusselt number increases with the decrease of porosity as can be seen in Figure (9 a-d), leading to high thermal performance. The reason for this is due to the heat transfer coefficient increasing with the decrease of porosity due to the reduction of surface

temperature of the microchip, leading to an increase of Nusselt number by removing the heat to the surrounding area through the porous media via natural convection. The heat transfer enhancement increases the cooling performance of the heat sink and thus increases the heat removal to the surrounding. As can be observed also, steel records the lowest Nusselt number because it contains low thermal conductivity which leads to low heat transfer enhancement.

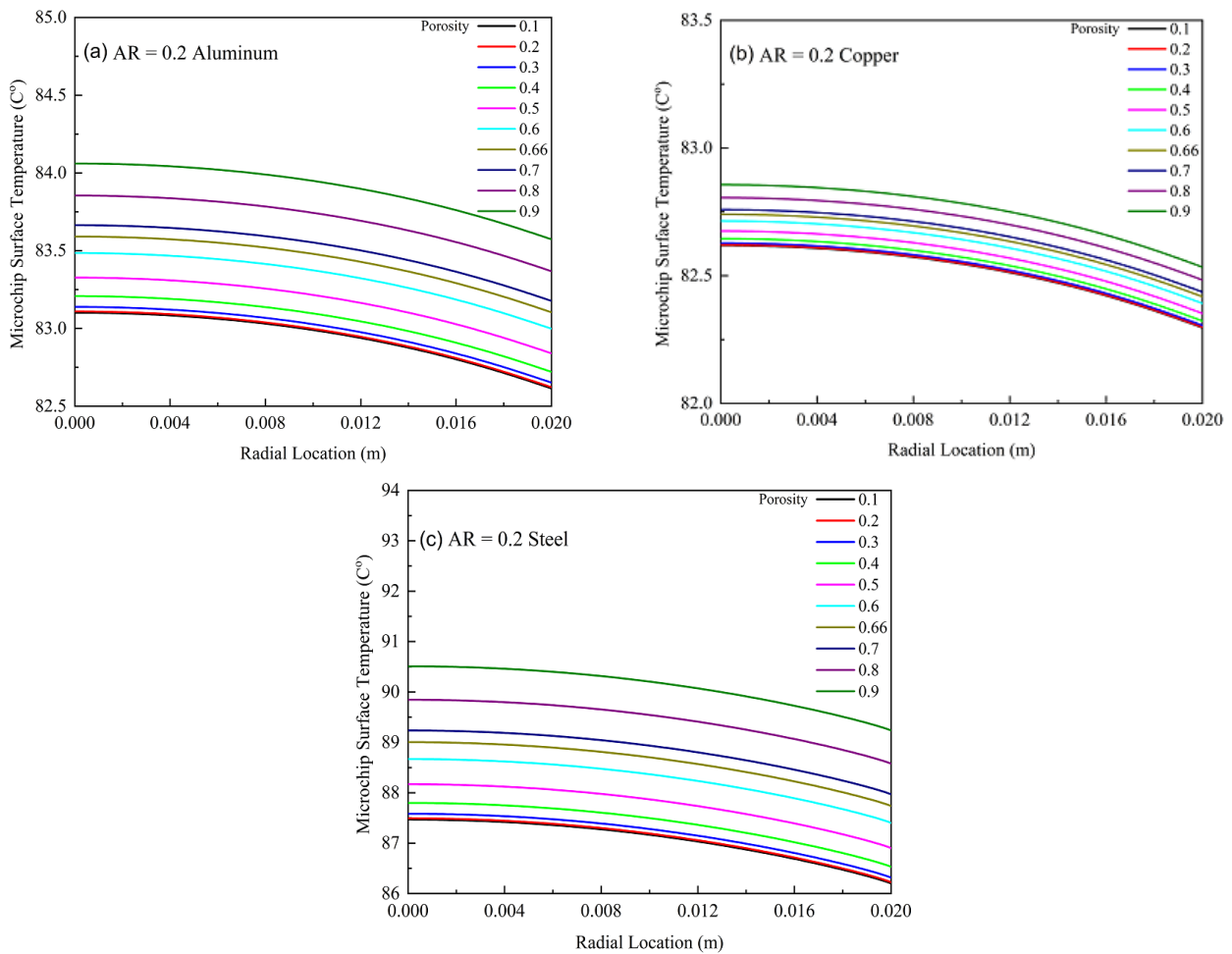


**Figure 8.** The influence of porosity on the surface temperature of the microchip at aspect ratio of 2 and porosity of 0.1 to 0.9.

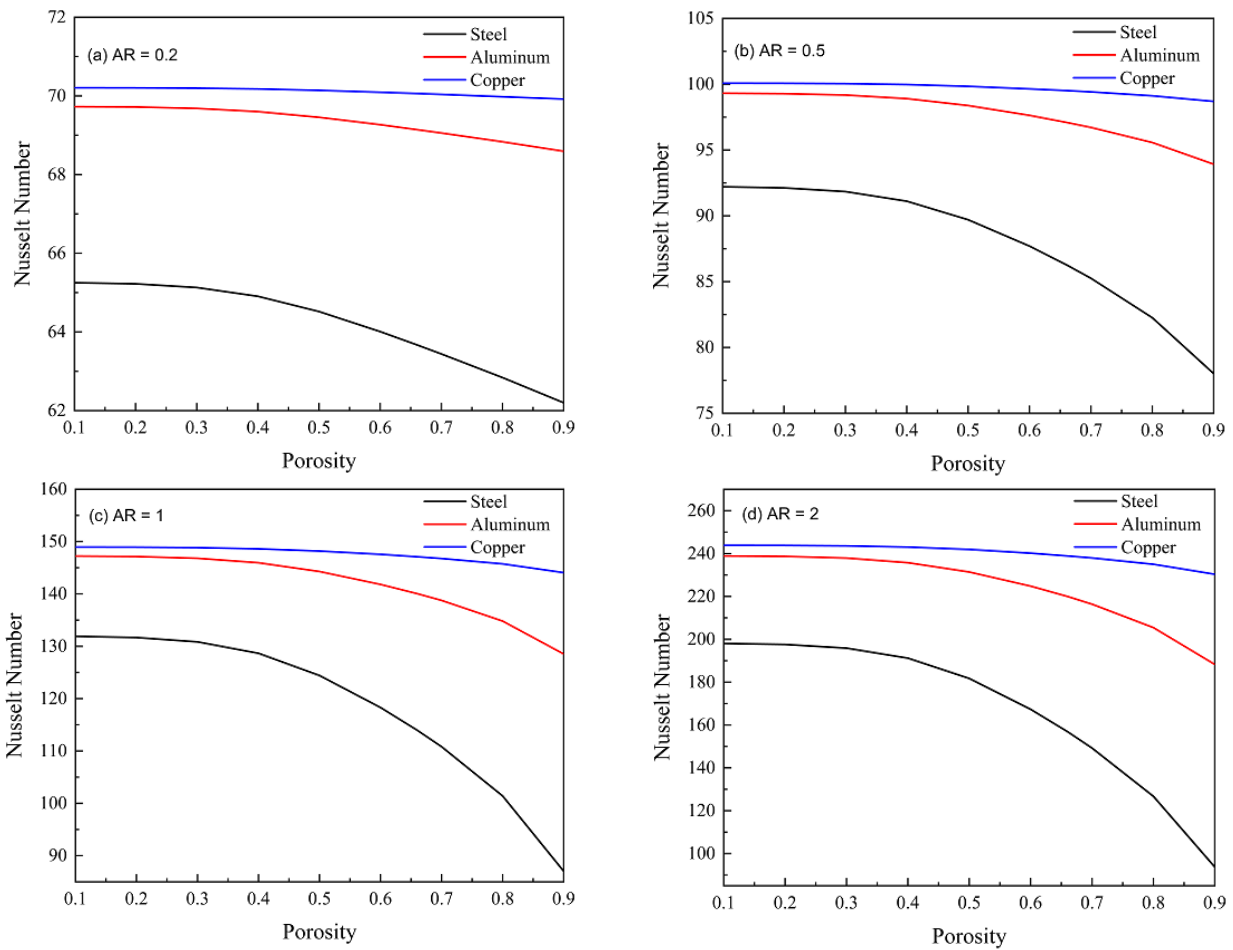


**Figure 9.** Nusselt number vs. porosity for steel, aluminium, and copper among four different aspect ratios for a range of values of porosity

#### 4. Conclusions

Numerical investigation is achieved to study the thermal behaviour of heat sink that is used to cool high powered microchips. Three metallic porous mediums were used in the study as heat sink (steel, aluminium, and copper) with two porosities (0.2, 0.4, and 0.8). Four aspect ratios of the heat sink were studied (0.2, 0.5, 1, and 2). The heat generated by the microchip of high power ( $>10^4$  W/m<sup>2</sup>) is removed to the ambient surroundings through the metal porous media by means of free convection heat transfer. Nusselt numbers were calculated and analysed. The model results show that copper is the best heat sink to be used compared to aluminium and steel. The surface temperature is at its minimum (41.58°C) at a porosity of 0.2 and AR = 2, leading to the highest Nusselt number (243.81). Steel shows the highest surface temperature

(89.35°C) at a porosity of 0.8 and AR = 0.2 which results in lowest Nusselt number (62.84). The effectiveness of the heat sink increases with the increase of aspect ratio. Nusselt number increases with the increase of aspect ratio and decreases with porosity for all metal porous mediums. Future research will focus on studying the problem in an experimental setting, as well as investigating the forced convection considering the variation of aspect ratio and porosity.

#### Nomenclature

- $\emptyset$  Porosity (-)
- $W$  Diameter (width) of the heat sink (m)
- $H$  Height of the heat sink (m)
- $h$  Height of the microchip (m)
- $w$  Diameter (width) of the microchip (m)
- $\mu$  Viscosity (Pa.s)

$\rho$	Density (kg/m <sup>3</sup> )
$K$	Permeability of porous media (m <sup>2</sup> )
$k$	Thermal conductivity of the porous media (W/m.K)
$c$	Heat capacity of the porous media (J/kg.K)
$C_f$	Forchheimer's constant (-)
$g$	Gravity (m/s <sup>2</sup> )
$\beta$	Thermal expansion coefficient of fluid. (1/K)
$d_p$	Mean particle diameter (m)
$D_e$	Equivalent diameter of the porous media (m)
$P$	Pressure (Pa)
$T$	Temperature (K)
$V$	Velocity (m/s)
Subscripts	
$f$	Fluid
$s$	Solid
$\infty$	Ambient
$eff$	Effective

## References

- [1] L. Gong, Y. Li, Z. Bai, and M. Xu, "Thermal performance of micro-channel heat sink with metallic porous/solid compound fin design," *Applied Thermal Engineering*, vol. 137, pp. 288-295, 2018.
- [2] N. Habib and M. Tahir, "Thermal analysis of proposed heat sink design under natural convection for the thermal management of electronics," *Thermal Science*, vol. 26, no. 2 Part, pp. 1487-1501, 2022.
- [3] A. Zehri *et al.*, "High porosity and light weight graphene foam heat sink and phase change material container for thermal management," *Nanotechnology*, vol. 31, no. 42, p. 424003, 2020.
- [4] E. M. Abo-Zahhad *et al.*, "A Micro-Metal Inserts Based Microchannel Heat Sink for Thermal Management of Densely Packed Semiconductor Systems," *Sustainability*, vol. 14, no. 21, p. 14182, 2022.
- [5] C. S. Sharma, G. Schlottig, T. Brunschwiler, M. K. Tiwari, B. Michel, and D. Poulikakos, "A novel method of energy efficient hotspot-targeted embedded liquid cooling for electronics: An experimental study," *International Journal of Heat and Mass Transfer*, vol. 88, pp. 684-694, 2015.
- [6] X. Chen, H. Ye, X. Fan, T. Ren, and G. Zhang, "A review of small heat pipes for electronics," *Applied Thermal Engineering*, vol. 96, pp. 1-17, 2016.
- [7] A. Arshad, H. M. Ali, W.-M. Yan, A. K. Hussein, and M. Ahmadlouydarab, "An experimental study of enhanced heat sinks for thermal management using n-eicosane as phase change material," *Applied Thermal Engineering*, vol. 132, pp. 52-66, 2018.
- [8] A. Kabeel, M. Mousa, M. M. Abdelaziz, R. Sathyamurthy, and M. Abdelgaied, "Performance of the novel design thermoelectric cooling system," *Heat Transfer*, vol. 49, no. 8, pp. 4134-4152, 2020.
- [9] M. A. Khan, H. M. Ali, T. u. Rehman, A. Arsalanloo, and H. Niyas, "Composite pin-fin heat sink for effective hotspot reduction," *Heat Transfer*, vol. 53, no. 4, pp. 1816-1838, 2024.
- [10] M. Hameed, H. N. Mohammed, and M. R. Abdullah, "The Improving the Thermal Performance of a Heat Exchanger using a New Passive Technology," *Tikrit Journal of Engineering Sciences*, vol. 30, no. 1, pp. 66-71, 2023.
- [11] T. K. Ibrahim, A. T. Al-Sammarraie, W. H. Al-Taha, M. R. Salimpour, M. Al-Jethelah, A. N. Abdalla, and H. Tao, "Experimental and numerical investigation of heat transfer augmentation in heat sinks using perforation technique," *Applied Thermal Engineering*, vol. 160, p. 113974, 2019.
- [12] T. K. Ibrahim, A. T. Al-Sammarraie, M. S. Al-Jethelah, W. H. Al-Doori, M. R. Salimpour, and H. Tao, "The impact of square shape perforations on the enhanced heat transfer from fins: Experimental and numerical study," *International Journal of Thermal Sciences*, vol. 149, p. 106144, 2020.
- [13] A. K. PV, G. C. AC, and P. M. Kamath, "Heat transfer enhancement of electronic chip cooling using porous medium," in *ASME Heat and Mass Transfer Conference*, 2013.
- [14] D. A. Nield and A. Bejan, *Convection in porous media*. New York: Springer, 2013.
- [15] T. K. Ibrahim, F. Basrawi, M. N. Mohammed, and H. Ibrahim, "Effect of perforation area on temperature distribution of the rectangular fins under natural convection," *ARPN Journal of Engineering and Applied Sciences*, vol. 11, no. 10, pp. 6371-6375, 2016.
- [16] T. K. Ibrahim *et al.*, "Experimental study on the effect of perforations shapes on vertical heated fins performance under forced convection heat

- transfer," *International Journal of Heat and Mass Transfer*, vol. 118, pp. 832-846, 2018.
- [17] M. Zaretabar, H. Asadian, and D. Ganji, "Numerical simulation of heat sink cooling in the mainboard chip of a computer with temperature dependent thermal conductivity," *Applied Thermal Engineering*, vol. 130, pp. 1450-1459, 2018.
- [18] Y. J. Lee and S. J. Kim, "Thermal optimization of the pin-fin heat sink with variable fin density cooled by natural convection," *Applied Thermal Engineering*, vol. 190, p. 116692, 2021.
- [19] H.-T. Chen, P.-L. Chen, J.-T. Horng, and Y.-H. Hung, "Design optimization for pin-fin heat sinks," 2005.
- [20] D. Yang, Y. Wang, G. Ding, Z. Jin, J. Zhao, and G. Wang, "Numerical and experimental analysis of cooling performance of single-phase array microchannel heat sinks with different pin-fin configurations," *Applied Thermal Engineering*, vol. 112, pp. 1547-1556, 2017.
- [21] J. Zhao, S. Huang, L. Gong, and Z. Huang, "Numerical study and optimizing on micro square pin-fin heat sink for electronic cooling," *Applied Thermal Engineering*, vol. 93, pp. 1347-1359, 2016.
- [22] P. Smakulski and S. Pietrowicz, "A review of the capabilities of high heat flux removal by porous materials, microchannels and spray cooling techniques," *Applied thermal engineering*, vol. 104, pp. 636-646, 2016.
- [23] L. Gong, J. Zhao, and S. Huang, "Numerical study on layout of micro-channel heat sink for thermal management of electronic devices," *Applied Thermal Engineering*, vol. 88, pp. 480-490, 2015.
- [24] T.-C. Hung, Y. Hung, and W.-M. Yan, "Design of Porous-Microchannel heat sinks with different porous configurations," *International Journal of Materials, Mechanics and Manufacturing*, vol. 4, no. 2, pp. 89-94, 2016.
- [25] T.-C. Hung, Y.-X. Huang, and W.-M. Yan, "Thermal performance analysis of porous-microchannel heat sinks with different configuration designs," *International Journal of Heat and Mass Transfer*, vol. 66, pp. 235-243, 2013.
- [26] T.-C. Hung and W.-M. Yan, "Thermal performance enhancement of microchannel heat sinks with sintered porous media," *Numerical Heat Transfer, Part A: Applications*, vol. 63, no. 9, pp. 666-686, 2013.
- [27] H. M. Ali, A. Arshad, M. Jabbal, and P. G. Verdin, "Thermal management of electronics devices with PCMs filled pin-fin heat sinks: a comparison," *International Journal of Heat and Mass Transfer*, vol. 117, pp. 1199-1204, 2018.
- [28] M. Al-Jethelah, H. Dheyab, S. Khudhayer, T. Ibrahim, and A. Al-Sammarraie, "Latent heat storage for hot beverages," *Journal of Mechanical Engineering and Sciences*, vol. 13, no. 3, pp. 5653-5664, 2019.
- [29] M. Arqam, L. S. Raffa, L. Clemon, M. S. Islam, M. Ryall, and N. S. Bennett, "Numerical and experimental investigation of a phase change material radial fin heat sink for electronics cooling," *Journal of Energy Storage*, vol. 98, p. 113113, 2024.
- [30] M. Motevalizadeh, A. Rooberahan, M. S. Namaghi, M. Mohammadi, M. Passandideh-Fard, and M. Sardarabadi, "Cooling enhancement of portable computers processor by a heat pipe assisted with phase change materials," *Journal of Energy Storage*, vol. 56, p. 106074, 2022.
- [31] R. Singh, A. Akbarzadeh, and M. Mochizuki, "Sintered porous heat sink for cooling of high-powered microprocessors for server applications," *International Journal of Heat and Mass Transfer*, vol. 52, no. 9-10, pp. 2289-2299, 2009.
- [32] R. Rachedi and S. Chikh, "Enhancement of electronic cooling by insertion of foam materials," *Heat and Mass Transfer*, vol. 37, no. 4-5, pp. 371-378, 2001.
- [33] K.-H. Ko and N. Anand, "Use of porous baffles to enhance heat transfer in a rectangular channel," *International Journal of Heat and Mass Transfer*, vol. 46, no. 22, pp. 4191-4199, 2003.
- [34] S. Y. Kim, J. W. Paek, and B. H. Kang, "Thermal performance of aluminum-foam heat sinks by forced air cooling," *IEEE Transactions on components and packaging technologies*, vol. 26, no. 1, pp. 262-267, 2003.
- [35] A. Bhattacharya and R. Mahajan, "Metal foam and finned metal foam heat sinks for electronics cooling in buoyancy-induced convection," 2006.
- [36] W. Hsieh, J. Wu, W. Shih, and W. Chiu, "Experimental investigation of heat-transfer characteristics of aluminum-foam heat sinks," *International Journal of Heat and Mass Transfer*, vol. 47, no. 23, pp. 5149-5157, 2004.
- [37] K. Leong and L. Jin, "Effect of oscillatory frequency on heat transfer in metal foam heat sinks of various pore densities," *International journal of heat and mass transfer*, vol. 49, no. 3-4, pp. 671-681, 2006.

- [38] C. T. DeGroot, A. G. Straatman, and L. J. Betchen, "Modeling forced convection in finned metal foam heat sinks," 2009.
- [39] Q. Wang, X. Han, A. Sommers, Y. Park, C. T'Joen, and A. Jacobi, "A review on application of carbonaceous materials and carbon matrix composites for heat exchangers and heat sinks," *International journal of refrigeration*, vol. 35, no. 1, pp. 7-26, 2012.
- [40] Y. Ould-Amer, S. Chikh, K. Bouhadeh, and G. Lauriat, "Forced convection cooling enhancement by use of porous materials," *International Journal of Heat and Fluid Flow*, vol. 19, no. 3, pp. 251-258, 1998.
- [41] M. E. Skuntz, R. Elander, M. Al Azawii, P. Bueno, and R. Anderson, "System efficiency of packed bed TES with radial flow vs. axial flow—Influence of aspect ratio," *Journal of Energy Storage*, vol. 72, p. 108463, 2023.
- [42] Ashrae, *ASHRAE Pocket Guide for Air Conditioning, Heating, Ventilation, Refrigeration*. ASHRAE, 2018.
- [43] F. P. Incropera, *Fundamentals of heat and mass transfer*, 6th ed. / Frank P. Incropera ... [et al.].. ed. Hoboken, NJ: Hoboken, NJ : John Wiley, 2007.
- [44] D. R. Pitts and L. E. Sissom, "Schaum's outline of theory and problems of heat transfer," Second Edition, 1998.
- [45] M. Fenni, M. Guellal, and S. Hamimid, "Influence of porosity properties on natural convection heat transfer in porous square cavity," *Physics of Fluids*, vol. 36, no. 5, 2024.